

# Phase imaging in reflection with the acoustic microscope

A. Atalar, C. F. Quate, and H. K. Wickramasinghe

Edward L. Ginzton Laboratory, Stanford University, Stanford, California 94305  
(Received 22 August 1977; accepted for publication 3 October 1977)

When a polished surface of a single crystal is examined with a converging acoustic beam the reflected signal has a characteristic response that is dependent upon the elastic properties of the reflecting surface. This property can be used in the acoustic microscope to monitor the thickness of layers deposited on these surfaces and the small-scale variations of the elastic parameters in these materials.

PACS numbers: 43.20.Fn, 43.35.Yb, 43.35.Sx, 68.25.+j

In our studies of the acoustic reflections from smooth surfaces of single crystals we have learned that various materials have a characteristic response determined by the elastic properties of the surface itself. We use the acoustic microscope to monitor this effect. We have determined that metallic, or dielectric layers, deposited on these surfaces alter this response in such a way that we can determine the thickness of these layers and locate some of the subsurface defects.

In the microscope<sup>1</sup> we use a strongly converging beam normally incident to the liquid-solid interface at the surface of the object. It has been our usual practice to record micrographs with the sample surface at the focal point of the beam. There the beam is more or less collimated and the returning signal has a maximum value. The details and contours of the surface are portrayed with moderate contrast, as expected from conventional imaging theory. What is unexpected, at least to us, is the fact that the smooth surfaces with different elastic parameters generate reflected signals that have a distinct characteristic for each material. This distinction shows up when the sample is translated along the axis of the beam toward the lens. There we find important differences in the profile of the reflected beam as compared to the mirrorlike reflections from a rigid surface.<sup>2</sup> At this interface the velocity difference is large, the critical angles are small, and much of the incident energy is totally reflected. In analyzing this problem we decompose the incident beam into an angular spectrum of plane waves with incident angles extending from 0° (normal incidence) to 50° (the half-width of the beam). Those rays with an incident angle that is larger than the critical angles undergo total internal reflection. They are reflected with an amplitude equal to that of the incident ray and with a phase shift that is determined by the ratio of the incident angle to the critical angle. These phase shifts—known as the Goos-Hanchen shifts in optics<sup>3</sup>—alter the focal properties of the returning beam in a way that is unique to each material. The relative phase shifts for the totally reflected rays will change in the presence of a thin film at the interface and this too can be easily observed at the output of the transducer. We believe that this mechanism can be used to explain the reversals in image contrast that have been observed by Wilson<sup>4</sup> in acoustic micrographs.

The geometry for the reflection microscope is depicted in Fig. 1. There element 1 is the piezoelectric transducer. It serves to convert the rf voltage across the film into a plane wave of sound propagating normal to the film. As a receiver for the wave reflected from

the sample it is sensitive to the phase of the returning wave. The output voltage is equal to the acoustic field of the returning pulse as integrated over the area of the transducer—an important feature of our system since we monitor and display the voltage amplitude,  $V$ . Element 2 is the acoustic lens which serves to focus the plane wave from the transducer into a waist at the focal point. Element 3 is the reflecting object that we want to characterize by translating this object along the  $z$  axis. Finally, we note that we use a 4-nsec pulse at the input and include a circulator to separate the input from the output. We also use time gating to separate the pulse reflected from the object from other spurious reflections.

We monitor the amplitude of the transducer voltage and record it as  $V(z)$  in order to distinguish this displacement along the axis of the beam from the lateral scanning that is used to record conventional acoustic micrographs. The  $z$  coordinate is measured from the focal point and positive values correspond to lens-object spacings greater than the focal length.

These curves for  $V(z)$  combine both the transducer response and the reflection characteristic of the object. We can separate these and analyze the transducer response by first assuming that the object is a rigid surface. The incident wave does not penetrate the interface of such an object and it is reflected as a mirror image. For this reflector the rf voltage across the transducer will reach its maximum value when the reflector is placed at the focal plane ( $z = 0$ ). When the

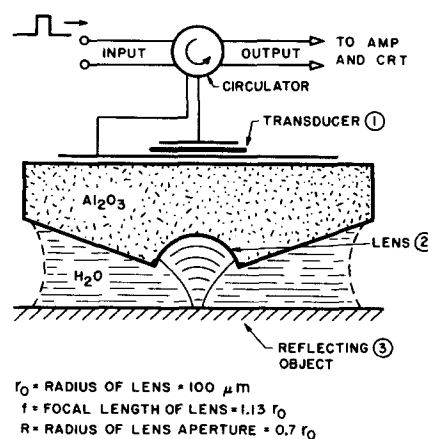


FIG. 1. The geometry of the acoustic transducer and lens as used for the reflection mode of the acoustic microscope.

sample spacing is decreased (negative  $z$ ) the reflected wave reaches the transducer in the form of a spherically diverging wave. There the transducer is excited with alternating regions of positive and negative phase and the integrated response is reduced. Similarly, the transducer response is reduced when the sample spacing is increased for then the reflected wave at the transducer is a converging spherical wave. If we neglect the transducer-lens spacing and assume that the system is lossless, we can work out a simple expression for  $V(z)$ . It is of the form  $\sin[\pi(R/f)^2 z/\lambda_0][\pi(R/f)^2 z/\lambda_0]^{-1}$ . The terms are defined in Fig. 1. For that lens this function with a maximum at  $z=0$  has a null at  $z = (f/R)^2 \lambda_0 = (1.13r_0/0.7r_0)^2 \lambda_0 = 2.6\lambda_0$ . The rigid reflector model has been used by both Weglein and Kompfner<sup>5</sup> to explain the contrast reversals that have been observed in micrographs of integrated circuits.<sup>4</sup> This model is inadequate since different elastic materials produce the same response and this does not conform to our observations. The rigid model, therefore, needs to be replaced with a reflector that is elastic.

We can modify the relation for  $V(z)$  given above by calculating the correct value for the reflectivity of the actual object. We begin as before by decomposing the incident beam into an angular spectrum of plane waves. Each of these plane waves is incident upon the interface with a different angle and we evaluate the amplitude  $r$  and the phase,  $\phi$ , of the reflectivity coefficient as a function of  $\theta$ , the angle of incidence. Plots of these two parameters for some simple crystals<sup>6</sup> immersed in water are shown in Fig. 2. We can see that the amplitude of the reflectivity coefficient is slightly less than unity when the incident angle is less than the critical angle and it is equal to unity for incident angles greater than the critical angle. The structure in this curve corresponds to the excitation of various modes in the solid.<sup>7</sup> It need not concern us since most of the energy is returned toward the lens. We are concerned, however, with the phase of the reflected rays. Those rays with small incident angles are reflected with a zero phase shift, while those rays with large incident angles are reflected with a phase shift that approaches  $2\pi$ . The information is contained in the phase of the reflected components, and with different materials and

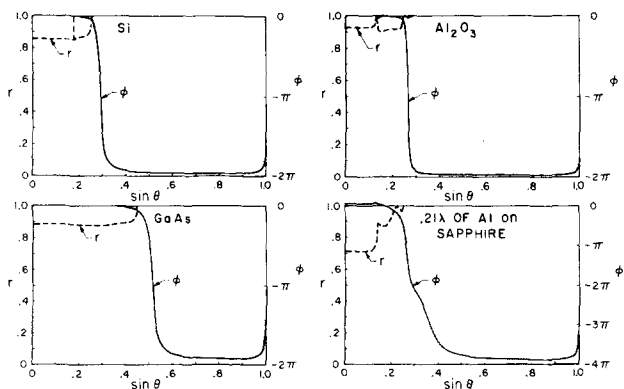


FIG. 2. The reflectivity for the labeled surfaces as a function of  $\sin \theta$  where  $\theta$  is the angle of incidence for plane waves. The reflection coefficient is given by  $r \exp(j\phi)$ . The amplitude and phase are plotted separately.

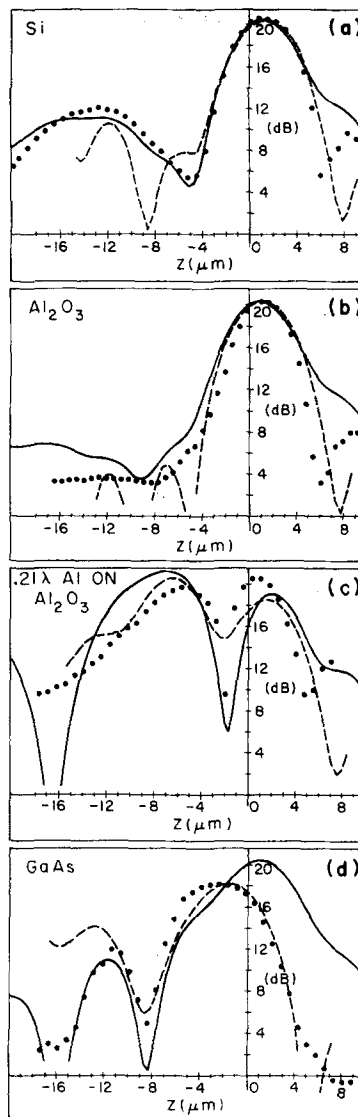


FIG. 3. The  $V(z)$  curves representing the transducer output versus the lens-object spacing,  $z$ . The dotted points are the measured response at 750 MHz. The dashed curves are from the computer program which includes loss in the liquid. The solid curves come from the paraxial ray equations with a lossless fluid.

different layering both the critical angle itself and the slope of the curve are altered.

These curves for the reflectivity coefficient, amplitude, and phase are used to characterize each surface and they are used in calculating the response of the output transducer. A computer program has been written for this purpose and the computed curves for the four materials given in Fig. 2 are shown as the dashed lines in Fig. 3. We have also used the *paraxial ray* approximation as a second approach to calculate the  $V(z)$  curve. There we assume that all of the waves in the Fourier decomposition intersect the  $z$  axis with a small angle. In a number of cases this gives a closed-form expression which adds a great deal to our physical insight. The calculated curves from the paraxial ray equations are shown as the solid lines in Fig. 3. The acoustic loss of the liquid has been neglected in these

curves. The measured results in Fig. 3 were recorded using a crystal with a transducer-lens spacing of 1.25 mm and the diffraction spreading of the beam over this length degrades the illumination of the lens. We suspect that this is the reason for the agreement between the paraxial ray equations and some of the experimental curves.

We have found in this study that the acoustic microscope can be used in conjunction with the axial translation of the sample to study the elastic properties of the surface on a dimensional scale that measures  $1 \mu$  in the lateral direction and  $1 \mu$  in depth. We believe that the information as gathered in this manner should be useful in studying subsurface defects, identifying different constituents that make up the surface in complex alloys, and in monitoring the layer thickness in fabricated microstructures. Although we have included no images here these curves do influence that work since small variations in the elastic parameters are more easily seen in the micrographs when the  $z$ -axis position coincides with the minimum of the curves of Fig. 3.

We want to express our appreciation to both R. G. Wilson and P. K. Tien for discussing their work with us prior to publication. This work was supported pri-

marily by the NBS/ARPA Program on Semiconductor Electronics and in part by the Joint Services Electronics Program (JSEP).

<sup>1</sup>R. A. Lemons and C. F. Quate, *Appl. Phys. Lett.* **25**, 251 (1974); C. F. Quate, *Semiconductor Silicon 1977*, Proc. Vol. 77-2, edited by H. R. Huff and E. Sirtl (Electrochemical Society, Princeton, 1977), p. 422.

<sup>2</sup>M. A. Breazeale has studied the reflection of acoustic beams from a water-steel interface and compared this with that from a water-aluminum interface. He finds that the profiles of the reflected beam are quite different. See M. A. Breazeale, L. Adler, and G. A. Scott, *J. Appl. Phys.* **48**, 530 (1977).

<sup>3</sup>M. McGuirk, C. K. Carniglia, *J. Opt. Soc. Am.* **67**, 103 (1977); **67**, 121 (1977); P. K. Tien, *Rev. Mod. Phys.* **49**, 361 (1977).

<sup>4</sup>R. G. Wilson, R. D. Weglein, and D. M. Bonnell, *Semiconductor Silicon 1977*, Proc. Vol. 77-2, edited by H. R. Huff and E. Sirtl (Electrochemical Society, Princeton, 1977), p. 431.

<sup>5</sup>R. D. Weglein and R. Kompfner (private communications).

<sup>6</sup>B. A. Auld, *Acoustic Fields and Waves in Solids* (Wiley-Interscience, New York, 1973), Vol. I, Table A.4.

<sup>7</sup>L. M. Brekhovskikh, *Waves in Layered Media*, edited by R. T. Beyer (Academic, New York, 1960), p. 34.

## Image resolution of the scanning acoustic microscope<sup>a)</sup>

R. D. Weglein and R. G. Wilson

*Hughes Research Laboratories, 3011 Malibu Canyon Road, Malibu, California 90265*  
(Received 7 February 1977; accepted for publication 3 October 1977)

We have measured the spatial frequency response of an experimental scanning acoustic microscope (SAM) at 375 MHz, using an acoustic high-resolution reflection test target consisting of Au bars on a silicon substrate. Although the instrument resolves 1.6- $\mu$ m line detail quite well, in favorable agreement with theoretical predictions, the shape of the spatial frequency response curve differs substantially from expectations.

PACS numbers: 43.35.Yb, 43.35.Sx, 06.50.Dc, 68.25.+j

The scanning acoustic microscope<sup>1</sup> (SAM) is a confocal coherent system, whose resolving power, assuming uniform aperture illumination, should be  $d_{\text{min}} = \lambda/4NA$ ,<sup>2</sup> where  $\lambda$  is the acoustic wavelength for compressional waves and  $NA$  is the numerical aperture.<sup>3</sup> Because of the inherently large  $NA$  of the acoustic system and because spherical aberration is virtually absent, the SAM resolving power is a small fraction of the acoustic wavelength. As an example, for a frequency of 375 MHz, two point objects spaced by 1.15  $\mu$ m should just be resolvable.

We have made preliminary measurements of the spatial frequency response of an experimental SAM. The work was motivated by our desire to (1) provide

experimental support to the theoretical predictions and (2) investigate the focused acoustic beam intensity profile (point spread function) as a function of frequency and axial distance from the focal plane. We describe the measurement technique and the resulting spatial frequency response curve in detail and comment on possible improvements in the SAM when operated at higher, yet still practical, microwave frequencies.

Our experimental SAM is a mechanically scanned system similar to that described in Ref. 1. Its acoustic lens, shown in Fig. 1, consists of a cylindrical  $C$ -axis sapphire rod, adapted at one end with a spherical depression<sup>3</sup> of half-angle  $\theta$  (approximately  $60^\circ$ ) and a 380- $\mu$ m radius. Recently, the transmission properties of the lens (spherical depression) have been improved substantially by applying a sputtered-glass acoustic  $\frac{1}{4}\lambda$  impedance transformer [an acoustic antireflection coating (AARC)].<sup>4</sup> The lens focuses 375-MHz incident longitudinal waves into a highly convergent acoustic

<sup>a)</sup>Research funded by the Advanced Research Projects Agency ORDER 2397 through the National Bureau of Standards Semiconductor Technology Program Contract No. 5-35898.